This is the accepted version of :
Urbani, M., Montanyá, J., van der Velde, O. A., Arcanjo, M., & López, J. A. (2022). Multi-stroke positive cloud-to-ground lightning sharing the same channel observed with a VHF broadband interferometer. Geophysical Research Letters, 49, e2021GL097272. https://doi.org/10.1029/2021GL097272

# Multi-Stroke Positive Cloud-to-Ground Lightning Sharing the Same Channel Observed with a VHF Broadband Interferometer

**M. Urbani[1], J. Montanyá [1], O. A. van der Velde[1], M. Arcanjo[1], J. A. López [1]**

[1]Electrical Engineering Department, Universitat Politècnica de Catalunya, Terrassa, Barcelona, Spain

**Key Points:**

- First time observation of positive cloud-to-ground strokes sharing the same channel to ground with a VHF broadband interferometer.
- A fast recoil leader and/or a fast breakdown connecting decayed leader channels play a crucial role in triggering the subsequent positive stroke.
- The high-resolution comparison between the first and subsequent stroke shows different VHF signatures related to the channel conductivity.

Corresponding author: Michele Urbani, michele.urbani@upc.edu

## Abstract

This work presents the first observation of a multi-stroke positive cloud-to-ground lightning flash sharing the same channel to ground mapped with a VHF broadband interferometer and a Lightning Mapping Array. This type of lightning flash is very rarely observed, and it is currently unclear how frequent it is and even under what conditions it occurs. Our observations indicate a scenario where the first downward positive leader initiates from a decayed negative channel. After the first return stroke, some of the main negative channel branches stop propagating and likely cut off. A fast recoil leader and/or a fast breakdown play a crucial role in reconnecting these previously decayed leader channels and initiating the subsequent positive stroke. The mechanism we propose to describe the phenomenon allows us to explain its rarity and the discrete positive charge transfer to the ground.



## Plain Language Summary

In the same lightning flash, whose usual duration is a few hundred milliseconds, there can be multiple negative cloud-to-ground (-CG) strokes with different terminations or following a pre-existing channel to the ground. In contrast, it is not common to have multiple positive cloud-to-ground (+CG) strokes, and especially multi-stroke +CG flashes sharing the same channel to ground are very rarely observed. This polarity asymmetry is not well understood and many aspects are debated. In this letter, we present for the first time the very high frequency (VHF) radio band observation of a multi-stroke +CG flash along the same channel, observed simultaneously by a VHF broadband interferometer and a Lightning Mapping Array (LMA) in north-central Colombia. These combined observations have a high temporal resolution and spatial accuracy and allowed us to observe in detail the development of flash and in particular to understand the initiation mechanism of the subsequent positive stroke.


## 1 Introduction

Positive cloud-to-ground (+CG) lightning flashes are less frequent than the negative counterpart, about 10% of the global cloud-to-ground lightning, but in general, their charge transfer is an order of magnitude greater (Rakov & Uman, 2003). For this reason, they usually can cause more damage in particular to tall structures like wind turbines (e.g., Montanyà et al., 2014; Becerra et al., 2018) or cause wildfire ignition (e.g., Fuquay et al., 1972; Blouin et al., 2016). Furthermore, +CG flashes are mainly associated with the production of transient luminous events like sprites in mesoscale convective systems (e.g., Boccippio et al., 1995; Williams et al., 2010; van der Velde et al., 2014). Therefore, +CG flashes have attracted great research interest in recent years and some aspects are still debated or require a better understanding.

One of these aspects is regarding the origin and the development of multi-stroke +CG lightning. Positive flashes usually have a single stroke (Rakov & Uman, 2003). However, several cases of multi-strokes positive flashes were recently studied and reported in the literature. The average number of strokes in a +CG flash is estimated around 1.0 and 1.3 and with a maximum multiplicity of 5 (e.g., Fleenor et al., 2009; Nag & Rakov, 2012; Wu et al., 2020). The first study reporting optical observations of multi-stroke +CGs flashes was conducted by Fleenor et al. (2009). They documented for the first time subsequent positive strokes sharing the same channel to ground, and observed nine multi-stroke +CG flashes of which five cases involving a pre-existing channel. Saba et al. (2010) reported high-speed video observations of 19 multi-stroke +CG flashes and only one case of subsequent positive stroke along the same channel. These optical observations highlighted the occurrence and rarity of the phenomenon, but present limitations in describing the flash development within the cloud and the mechanisms that make subsequent positive strokes possible.

Thanks to improved lightning detection systems, new observations and findings on multi-stroke +CG flashes are emerging. Wu et al. (2020) reported 47 new observations of multi-stroke +CG flashes during the winter season in Japan. They observe that downward positive leaders (DPLs) in multi-stroke flashes are mostly originated from in-cloud negative leader channels. It is relevant to note that they did not observe any subsequent stroke striking at the same location as a previous stroke. Yuan et al. (2020) investigated the origin of an uncommon three-stroke event with different terminations to ground and proposed a mechanism involving an advancing negative leader.
Recently, Zhu et al. (2021) observed 84 multi-stroke +CG flashes during a supercell storm in Argentina. They observed 54 (64%) +CG flashes with a subsequent leader following a pre-existing channel to ground, assuming that two different strokes share the same channel if their striking points are within 100 m. They suggested that the behavior of subsequent leaders in positive lightning can be very similar to subsequent leaders in negative lightning. These new observations raise interest and new questions about the conditions necessary for these phenomena to occur, and what mechanisms may explain the discrete charge transfer along the same channel in +CG flashes.

The VHF broadband interferometer is a privileged instrument for investigating this phenomenon. It has a very high temporal resolution, at least one order of magnitude higher than other lightning detection networks with remote sensors, and its strength is the capability to resolve in detail leader channels and breakdown discharges even inside the cloud. To the best of our knowledge, this is the first time that a multi-stroke +CG lightning flash sharing the same channel to ground was observed by a VHF broadband interferometer and simultaneously by a Lightning Mapping Array (LMA).

## 2 Instrumentation and Methodology

The data presented in this work were recorded during an observational campaign at the Universidad Industrial de Santander (UIS) campus of Barrancabermeja (Colombia) in autumn 2019. Instruments, processing techniques, and the deployment of the instrumentation are further described by Urbani et al. (2021).

### 2.1 VHF Broadband Interferometer

A VHF broadband interferometer (INTF) is an instrument capable of mapping lightning discharges with a high temporal resolution. We designed and built our version, which consists of three antennas (aluminum disks of radius 20 cm) deployed along two orthogonal baselines of 22 m. The antenna's output signal is connected to a bandpass filter (20-80 MHz) and then preamplified. The digitizer used for the acquisition system is a GaGe Razor Express 1604 with four channels, 16-bit resolution and 200 MS per second sampling rate. The interferometric processing technique is a window-based cross-correlation method (Stock et al., 2014) improved by a clustering algorithm to average overlapping solutions and perform noise reduction (Urbani et al., 2021). The time window used is 512 samples (2.56 ns), the timing uncertainty and the angular resolution are reported in the Supporting Information (SI).

### 2.2 Colombia Lightning Mapping Array

The Colombia Lightning Mapping Array (Colombia-LMA) was installed by the Universitat Politécnica de Catalunya (UPC) lightning research group (López et al., 2019). At the time of the measurements, it consisted of 8 VHF antennas (60-66 MHz bandwidth) deployed with baselines from $\sim 6$ to $\sim 36$ km around the city of Barrancabermeja. The processing technique based on time-of-arrival is provided by New Mexico Tech. More detailed information about the LMA can be found in Rison et al. (1999) and Thomas et al. (2004).

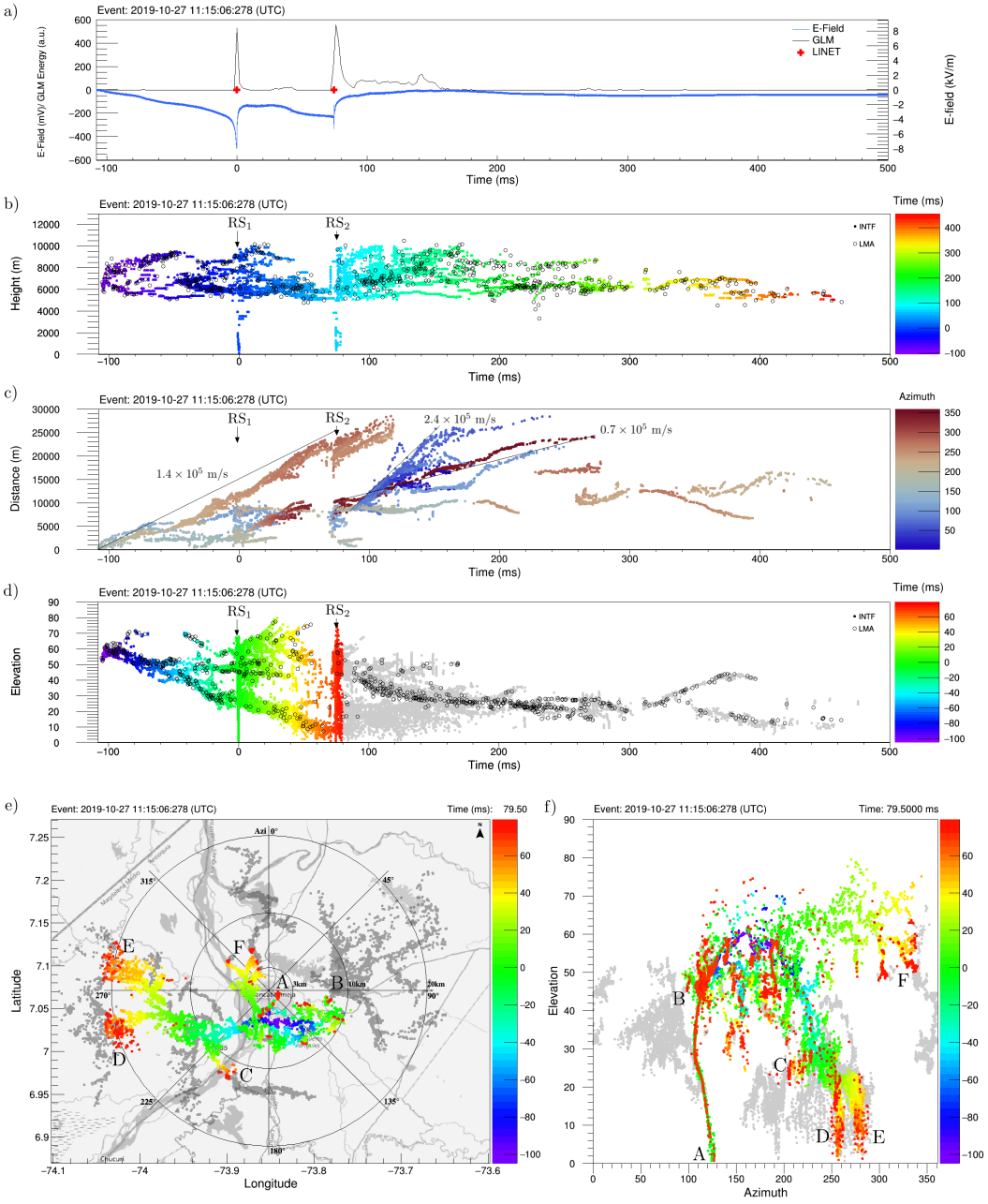


**Figure 1.** Multi-stroke +CG flash along the same channel, event: 2019-10-27 11:15:06 (UTC). a) Electric field waveform recorded by the flat plate antenna, LINET detection (Betz et al., 2009) and Geostationary Lightning Mapper (GLM) energy (Goodman et al., 2013). b) Evolution of the multi-stroke +CG flash in altitude, Quasi-3D data. c) Time-distance plot of the VHF sources from the lightning initiation, colored by azimuth, Quasi-3D data. d) Time-elevation plot INTF data compared with LMA data. e) Development of the flash, Quasi-3D data. f) VHF broadband interferometer data on Elevation-Azimuth plane. It is possible to observe (see letter A) the subsequent positive stroke (red) along the same pre-existing cloud-to-ground channel (green). The correspondence between panels e) and f) is highlighted through the letters A-F. An animation of the entire flash is available in the Supporting Information.

### 2.3 Quasi-3D conversion

Simultaneous detections of a lightning flash with the INTF and the LMA allow us to use a post-processing technique, which has the great advantage of combining the high temporal resolution of the INTF with the spatial accuracy of the LMA. This technique called "Quasi-3D conversion" was introduced and described by Stock (2014). It consists of an interpolation technique in a few steps: first, the projection of the LMA data on the system of reference of the interferometer; second, a raw approximation of the 3D projection is made for each INTF source in the elevation-azimuth plane by interpolating the values to the LMA sources; finally, an iterative procedure using alternately the spatial correlation and successive projections allows an estimation of the radial distance of individual INTF sources.
This technique is clearly approximated and imperfect because in some cases there simply are not enough LMA sources to reconstruct the correct development of all lightning branches (or very fast lightning processes) and sometimes this may introduce artifacts. A noise reduction and supervised processing are needed to get reliable results. On the other hand, Quasi-3D reconstruction adds substantial information to understand the overall structure of the flash removing the typical ambiguity in the 2D data of the interferometer. It can be appreciated in Figure 1e and Figure 1f, where a correspondence between different leader branches is highlighted through the letters A-F.

## 3 Observations and Analysis

We observed two multi-stroke +CG flashes with a double stroke along the same channel to ground, named with the timestamp in UTC time of the first return stroke: (1) 2019-10-27 11:05:10 and (2) 2019-10-27 11:15:06. We present in detail only the second flash for sake of brevity, but where some differences are relevant or some important results are consistent we mention the other case.

### 3.1 Multi-stroke +CG flash: 2019-10-27 11:15:06

In this section, we describe the development of the multi-stroke +CG flash (2), which can be best appreciated from the Quasi-3D data animation provided in the SI. A frame of this animation and the evolution of the main physical quantities and dimensions are shown in Figure 1. Additionally, a schematic representation of the flash development is provided in Figure 2.

The origin of the flash (2) was located by the LMA at an altitude of around 6 km and a horizontal distance from the INTF of about 4.5 km.
After an initiation phase, of which the duration is around 1.5 ms propagating upward, several negative leader branches start growing with an average speed of $1.2 \times 10^5$ m/s in two main directions upward and horizontal (Animation S1, Figure 2a). The strong VHF emission of the negative leaders masks the positive leader development, and only a faint emission belonging to the positive leaders can be clearly located at a height of around 5.5 km after 31 ms from the initiation. The upward negative leader subsequently forks again and both branches stop propagating about $\sim$ 40 ms before the first positive stroke, reaching an altitude of around 10 km. A third negative branch initiates from one of the previous vertical branches at an altitude of 7.5 km and propagates upward with a similar speed. The main horizontal negative leader branch grows westward, generating multiple secondary branches.

According to our best interpretation of the data (Figure S3, Figure 2c), it seems that the DPL does not originate from the typical bidirectional leader development after the flash initiation (e.g. Mazur, 2002; van der Velde et al., 2014; Li et al., 2020), but from the negative horizontal channel in its lowest altitude location ($\sim$5.7 km). A similar scenario is widely reported in literature (e.g. Krehbiel, 1981; Saba et al., 2009; Nag & Rakov, 2012;

Wu et al., 2020; Yuan et al., 2020). In our data, it is possible to observe a recoil leader along a decayed secondary branch of the horizontal negative channel simultaneously with the DPL initiation. This could be evidence of a disconnected channel and it might create the conditions to initiate the first DPL (Figure 2b, Figure S3). The DPL initiates about 4.8 ms before the first return stroke (RS1). The development of the DPL is mainly vertical (the horizontal development is around 3.2 km) with an overall average speed of $1.4 \times 10^6$ m/s. More details on the initiation of first DPL are reported in the SI.

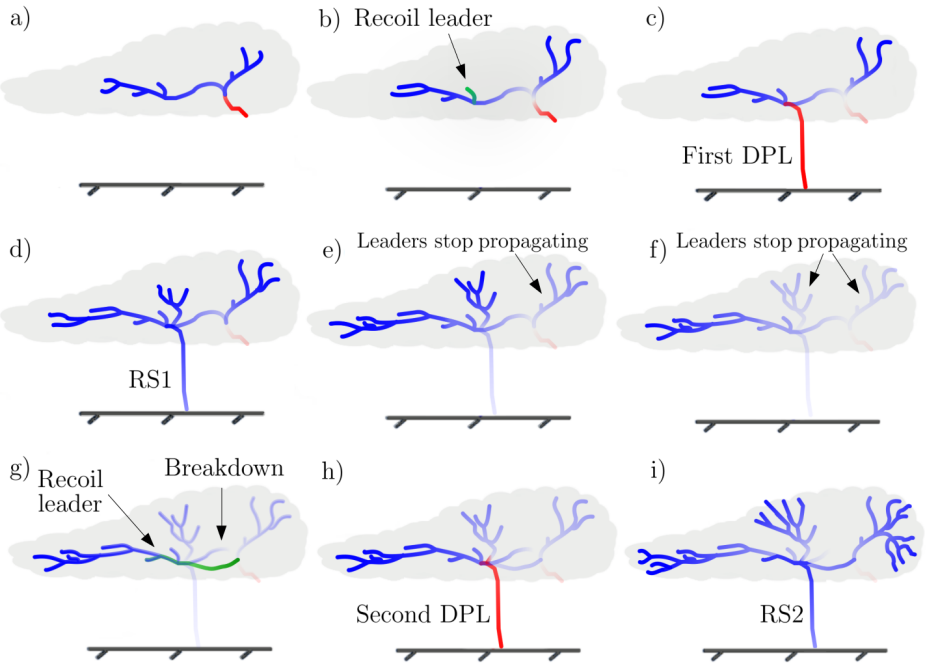


**Figure 2.** Schematic illustration of the multi-stroke +CG flash 2019-10-27 11:15:06. Blue lines and red lines indicate respectively propagating negative leaders and propagating positive leaders (observed by the INTF). Green lines indicate fast lightning processes such as recoil leaders or fast new breakdowns. The gradient color indicates time evolution and the faded color indicates decayed channels which are no longer propagating.

After the DPL connection with the ground, the return stroke RS1 brings ground potential to the channel, inserting negative charge along the previous negative leader channels. The vast majority of leader channels are involved, but there is more VHF activity in the horizontal channel compared with the vertical ones and the initiation of another main negative leader branch in a different direction (Figure 1e, negative leader branch F, Figure 2d). After RS1, the flash continues to propagate in the two negative horizontal branches of the leader, the westward branch and the new northward branch. After 40 ms from RS1, all leading upward branches to the east stop propagating (Figure 2e), and after 58 ms from RS1, the northward branch (F) stops propagating, while the westward branch (D,E) continues to propagate reaching a length of about 25 km (Figure 2f). Approximately 2 ms before the second return stroke (RS2), a fast recoil discharge can be observed which appears to involve or possibly trigger the subsequent DPL (Figure 2g). More details on this fast process and the initiation of the second DPL along the previous channel to ground are discussed in section 3.2. The interstroke interval between the RS1 and RS2 is about 74.5 ms, whereas in flash (1) it is about 25.5 ms.

Similarly, after the RS2, it is possible to observe a burst of VHF activity that can be associated with the continuing current phase (e.g. Lapierre et al., 2017). The continuing current can also be seen from the Geostationary Lightning Mapper (GLM) data and the electric field measurements (Figure 1a).
Figure 1e shows the increase in VHF activity especially in the westward horizontal branches (C,D,E) and in the previously stopped northward branch (F), where the fast processes (red color) correspond to the re-ionization of the leader tips, an effect of the continuing current. Negative branch Leader (F) restarts to propagate again after RS2 (Figure 2i). A new leader branch (B) is initiated after 15 ms from RS2 giving rise to a particularly extended and branched negative leader with higher speed $2.4 \times 10^5$ m/s, probably developing in a previously highly ionized area.

### 3.2 Initiation of the subsequent positive leader along the previous channel

One of the main questions regarding multi-stroke +CG flashes is how the subsequent downward positive leader could initiate and propagate along the same channel of the first DPL and why this is not as common as in -CG flashes. To investigate this aspect, we analyze what happens in the last milliseconds before the second return stroke. In this section, we describe the observations and the analysis for the multi-stroke +CG flash (2) illustrated in Figure 3, the other case is reported in the SI. The interpretation of these observations are discussed in section 4.

Figure 3a is an overview of the data collected in the last 4 ms before RS2. It shows a time-elevation plot with the VHF sources detected by the INTF and the LMA, the VHF waveform, and the electric field waveform detected by the flat plate antenna. It can be seen that a fast recoil leader [A] starts to propagates at about 2.4 ms before RS2. After 0.5 ms, it initiates a breakdown phase [B] and then it continues to propagate likely retracing a previous channel [C] until about 1.5 ms before RS2. In Figure 3b and 3c, we map with an elevation-azimuth plot the propagation of the leader stages [A] and [B], whereas in Figure 3d we consider a larger time interval including [C].

The analysis of these observations provides a more complete description of the recoil leader and the breakdown preceding the second DPL. We observed that the recoil leader initiates from the far end of a secondary decayed branch belonging to the main horizontal negative leader branch. This secondary branch was the one likely involved in triggering the first DPL (Figure S3) and it was subsequently extended by RS1 (Animation S1). The recoil leader retraces the channel propagating backward (Figure 3b). Although we are not able to precisely localize the three-dimensional development of this branch, the fact that it proceeds from a lower to a higher elevation suggests that the recoil leader is approaching, in the INTF reference system. This assumption is also supported by the increase of the VHF intensity and the monotonic enhancement of the electric field detected by the flat plate antenna in time correspondence with the recoil leader stage [A] as indicated by a black arrow in Figure 3a. The combined observations of the leader's spatial development and the electric field enhancement allow us to infer the leader charge polarity which is consistent with an approaching negative leader. The recoil leader speed was estimated to be between $1.0 - 1.5 \times 10^7$ m/s by a comparison with the speed of the previous negative leader ($1.2 \times 10^6$ m/s) along the same channel.

After 0.5 ms, we observed a strong increase of the VHF intensity and a variation in the electric field consistent with a fast breakdown [B], which likely reconnects previously disconnected leader channels. According to what we can see with INTF, it is interesting to note that it does not seem to retrace a previous channel but it traces a new path connecting itself with the origin of the flash (Figure 3b and 3c). After the connection with the origin of the flash, another recoil leader [C] can be observed, likely the continuation of [A] and [B], in a decayed leader branch clearly not belonging to the main horizontal leader channel. When the recoil leader [C] stops propagating, it can be observed in the electric field waveform the

indication of an accumulation of positive charge which gives rise to the second DPL in the following 0.3 ms. The second DPL is shown in Figure 4c and 4d and it is described in detail in the next section.

Finally, we show in Figure 3e the first 300 microseconds after the second DPL connection to the ground. It is possible to map the RS2 retracing the DPL channel and moreover, it is interesting to note that the whole in-cloud VHF activity during this time interval is located around the recoil leader A-C. Especially, as indicated by the arrows, along the the recoil channel [A], then in [C] and in the junction point between [A] and [B] from where it originates a new fast negative leader channel. These observations seems to support the hypothesis that the recoil leader A-C is not an uncorrelated lightning process happening before RS2 but probably the trigger mechanism of the subsequent DPL.

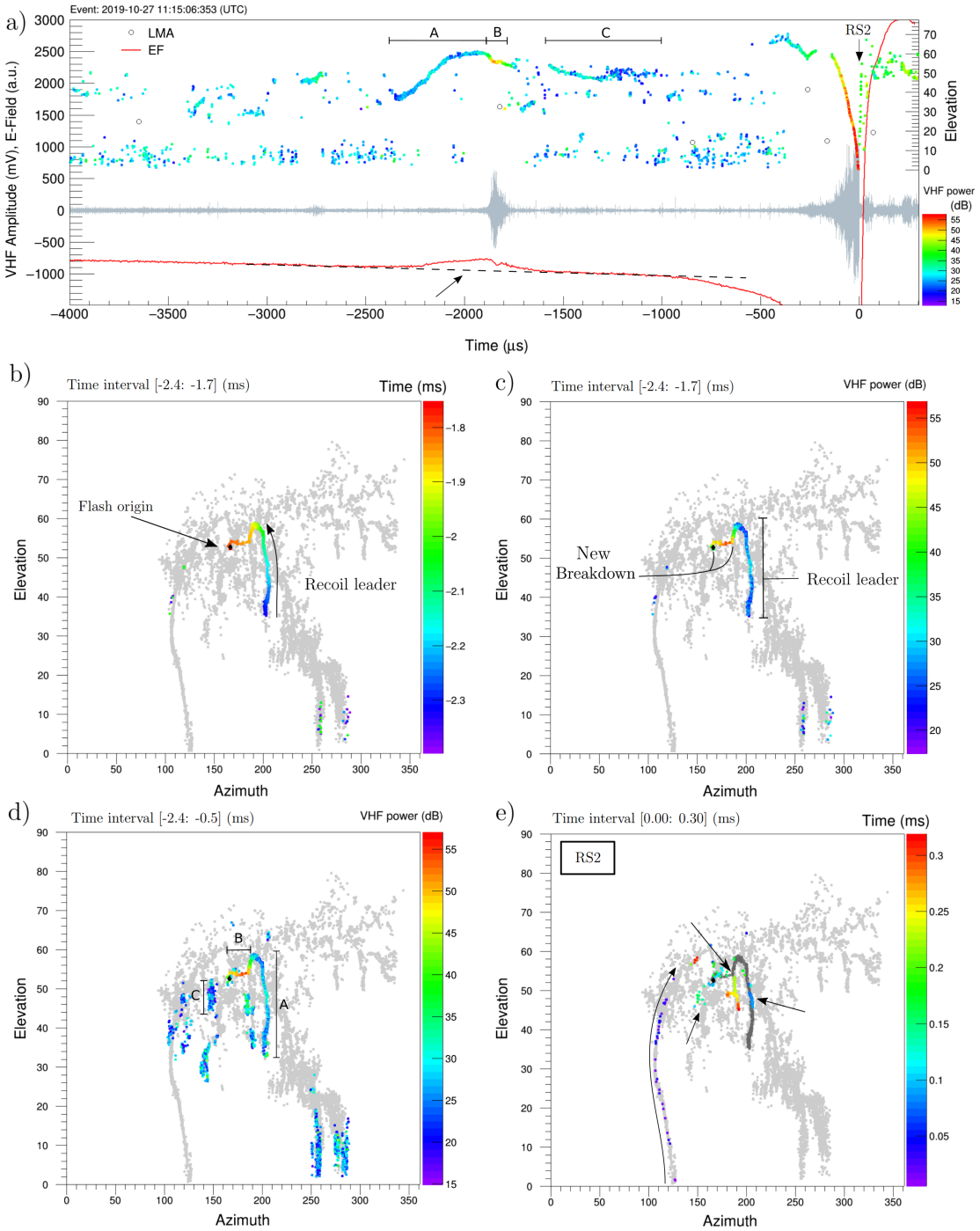


**Figure 3.** Initiation of the second DPL along a previous channel to ground, multi-stroke +CG flash 019-10-27 11:15:06 (UTC). a) Overview of the last 4 ms before RS2. Time-elevation plot of the VHF sources mapped by the INTF and LMA. Electric field waveform (red line) recorded by the flat plate antenna and VHF waveform (gray line). A black arrow indicates the electric field enhancement in correspondence of the approaching recoil leader. b) and c) Recoil leader and new breakdown connecting a previous channel end to the flash origin. Respectively colored by time and VHF power. d) Elevation-azimuth map of the leader channels A-C. e) VHF sources in the subsequent 300 microseconds after the DPL connection to the ground. It is relevant to note VHF activity near the previous leader channels A-C.

### 3.3 Comparison between the first positive stroke and the subsequent stroke.

The striking point of the event (2) was about 1.2 km away from our INTF location. The accuracy of this location is good because LINET detected both positive strokes and provides compatible values (same longitude: -73.8412 and latitude: 7.0674 and 7.0670). Furthermore, the INTF mapping confirm they have the same channel and same striking point. According to LINET, the peak current of the first positive stroke is 52.2 kA and the subsequent 20.7 kA and the time elapsed between them is about 75 ms.

In Figure 4, we provide an unprecedented high-resolution comparison between the first positive stroke and the subsequent stroke. Figure 4a shows only the last 750 $\mu s$ of the first DPL, while the total duration was 4.8 ms, and the return stroke process RS1. Panel b) shows the elevation-azimuth map, the VHF sources in dark grey color correspond to the total duration of the DPL, except the last 750 $\mu s$ that are colored according to the time evolution. In the background, the VHF sources in light gray color show the flash development before RS1. Figure 4c shows the total duration of the subsequent DPL (350 $\mu s$) and the return stroke process RS2. The subsequent DPL is more intense in VHF and it allows to clearly identify the origin of the subsequent positive stroke. The origin of the subsequent positive stroke is likely the same as the first DPL, which is from a previous horizontal negative leader channel in the lower altitude location (Figure 4b and 4d).

It is particularly interesting to note the different VHF signatures of the two DPLs. The first DPL is propagating in virgin air with a quite constant 2D speed of $1.5 \times 10^6$ m/s in the last 750 $\mu s$ before RS1. The VHF waveform presents an intermittent pattern of bursts of VHF pulses with an evident periodicity, every 10-20 $\mu s$, located on the positive leader tip. A similar observation of this intermittent pattern was recently shown by Pu et al. (2021). Further analysis of the VHF bursts and the DPL propagation is reported in the SI.
The subsequent DPL is faster, following a pre-ionized channel, its average 2D speed is quite constant at $1.3 \times 10^7$ m/s and slightly accelerating in the last 20 $\mu s$ to $2.0 \times 10^7$ m/s. This speed range is very similar to the speed of dart leaders following negative CG strokes (e.g., Urbani et al., 2021) and the recent measurements of (Zhu et al., 2021). In the subsequent DPL, it is not possible to clearly distinguish any intermittent pattern, this could be due to the higher speed or different propagation conditions along the pre-existing channel.

Another remarkable observation is regarding the VHF waveform of the return strokes (Figure 4a and 4c). The first RS has a more intense VHF signal and a 2D speed of $5.1 \times 10^7$ m/s while in the second case the signal amplitude is much weaker and the 2D speed is higher, about $1.23 \times 10^8$ m/s. It is interesting to note that despite the higher speed and the weaker signal, the INTF was able to better map RS2 than RS1, which suggests that in RS1 more sources were simultaneously emitting (along the channel or in different branches) while in RS2 what has been mapped is the wavefront of the return stroke (Figure 3e). We suggest that the different VHF signatures between the first and the subsequent return stroke could be due to the different conductivity of the channel, higher in RS2 than RS1.

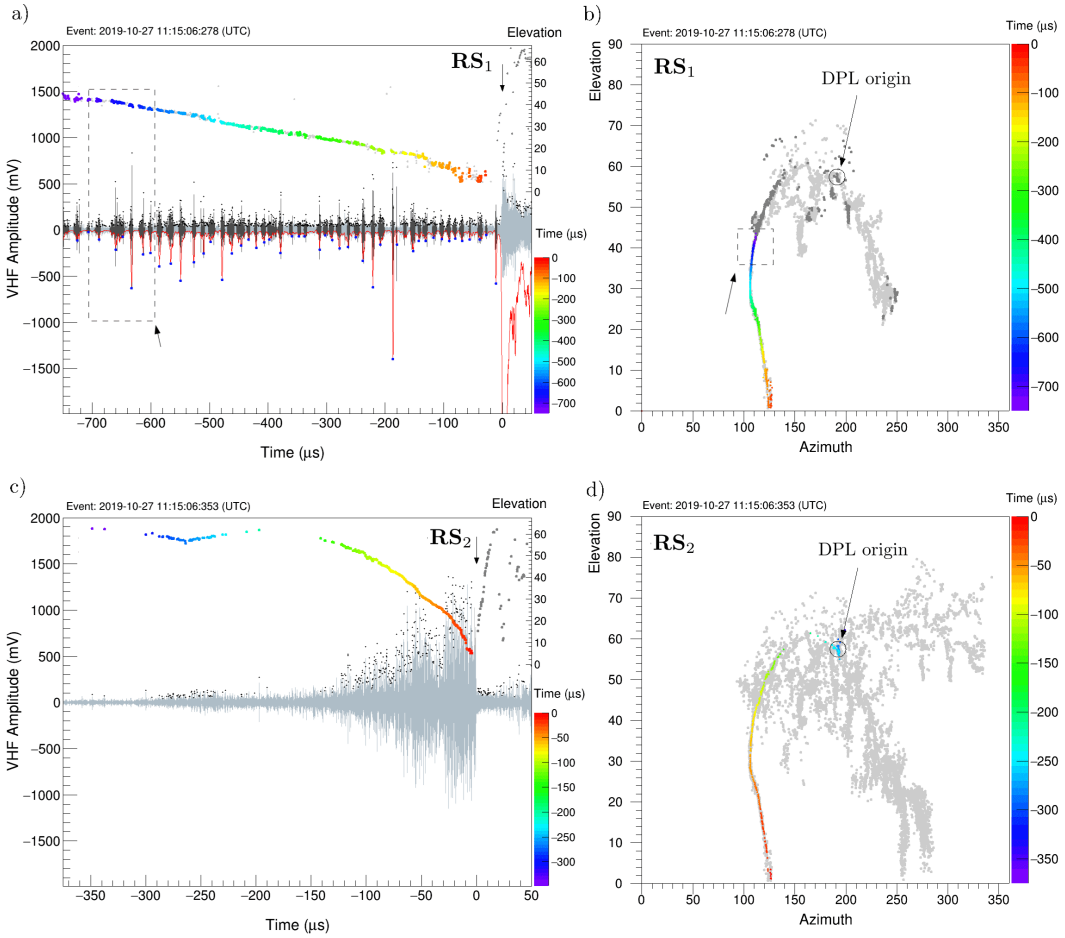


**Figure 4.** Comparison between the first and the second positive strokes of the multi-stroke event: 2019-10-27 11:15:06 (UTC).

a) VHF waveform and sources mapped by the VHF broadband interferometer (INTF) of the first positive stroke. The intermittent pattern of VHF is highlighted through two different shades of gray, an average envelope (red line) and its local maxima of the magnitude (blue dots). b) Elevation-Azimuth map of the VHF sources located by the INTF, c) VHF waveform and sources mapped by the INTF of the second positive stroke. d) Elevation-azimuth map of the VHF sources located by the INTF.

## 4 Discussion

The recent observations by Zhu et al. (2021) by means of the low/high frequency with the Córdoba Argentina Marx Meter Array (CAMMA) suggest that the processes in positive flashes with multiple strokes to ground sharing the same channel appears very similar to the mechanism in -CG flashes but with opposite polarity. Their observations belong to a supercell storm anomalously charged with the main negative charge region located above the main positive charge region. They observed that the positive subsequent strokes were initiated from the decayed in-cloud negative branches near their far ends by recoil leaders. In the three-stroke +CG flash presented by Zhu et al. (2021), they were able to map the positive recoil leader propagating backward, with a duration of more than 10 ms.

Similarly to Zhu et al. (2021), we observed that subsequent strokes occur after some negative leader branches stop propagating. Therefore, the presence of decayed negative channels seems to be a key aspect in multiple positive strokes. We also observed a recoil leader initiated from the far end of a decayed leader channel, but in our case it is a much faster process (speed $10^7$ m/s and duration of 1.8 ms) and according to our analysis the recoil leader polarity seems to be negative. In both flashes we recorded, we observed a fast breakdown a few hundred microseconds before the second DPL initiation, respectively, 200 microseconds for flash (1) and 1.8 milliseconds for (2). The observation of this fast breakdown along a new channel path, described in section 3.2, has never been reported before. Our interferometer and LMA data do not show a slow positive recoil leader of several milliseconds before the subsequent return stroke as observed by Zhu et al. (2021), but this is not necessarily in contradiction with their observations. Our instrumentation operates at a higher frequency radio band and it is more suited to detect breakdown and streamer activity near the head of propagating leaders instead of in-cloud current pulses. Therefore, we do not exclude that a slow positive recoil process like the one described by Zhu et al. (2021) could occur along one of the cut-off negative leaders during stage (f) in Figure 2, while their instrument does not resolve the very fast process we observed during stage (g).

We propose an alternative interpretation of our data, which does not require a slow positive recoil leader, but still involved the presence of decayed channels that cut-off after the first return stroke (Figure 2e and 2f). The evidence of this disconnection is found in the fast breakdown observed in the two milliseconds before the DPL (Figure 3). We assume an accumulation of positive charge at the root of one of the previous negative leaders, during stage (f), to explain the negative recoil leader we observed in opposite direction of a propagating negative leader branch. The fast breakdown acts as a switch that reconnects the decayed leader channel branches and allows the positive charge to propagate downward in the pre-existing return stroke channel to ground (Figure 2g and 2h). In this scenario, the positive leader occurs after the trigger mechanism, and is much faster in time (two order of magnitude) than what was observed by Zhu et al. (2021). Actually, our observations have similarities to the two-stroke +CG flash shown by Zhu et al. (2021) in their figure 4, where a slow positive recoil leader is not evident and it might be an indication of a fast breakdown before RS2, as it can be seen in the electric field waveform.

This mechanism might explain why the multi-stroke +CG flashes through the same channel are rare. The reason could be that usually in single stroke +CG flashes the DPL originates from the bi-directional flash initiation (e.g., van der Velde et al., 2014), whereas in multi-stroke +CG flashes the DPLs mostly originate from in-cloud negative leader channels (Wu et al., 2020; Yuan et al., 2020). Furthermore, the condition of sharing the same channel to ground instead of initiating a new DPL may be subordinated to the possibility of a re-connection with a decayed channel through a fast recoil leader and/or a breakdown.
The available cases suggest that this type of +CG flash requires more than one main negative leader branch near the flash origin and first stroke location. The cutoff must occur within tens of milliseconds after the first return stroke in order to maintain conductivity of the channel to ground for it to be re-used. These condition may not be facilitated in all storms.

Due to the scarcity of similar observations, the data presented are particularly valuable in describing the multi-stroke +CG flashes along the same channel. Likely not one single mechanism is able to explain each occurrence. Further studies and observations will lead to a more complete understanding of this phenomenon.

## Open Research

Measurements and data file supporting the conclusions are available at:
https://doi.org/10.7910/DVN/YUWYRD

**Acknowledgments**
This project has received funding from the European Union's Horizon 2020 research and innovation program under the Marie Sklodowska-Curie grant agreement 722337.
The authors are grateful to Keraunos (Colombia) for providing LINET data.

## References

Becerra, M., Long, M., Schulz, W., & Thottappillil, R. (2018). On the estimation of the lightning incidence to offshore wind farms. *Electric power systems research*, *157*, 211–226.

Betz, H. D., Schmidt, K., Laroche, P., Blanchet, P., Oettinger, W. P., Defer, E., ... Konarski, J. (2009). Linet—an international lightning detection network in europe. *Atmospheric Research*, *91*(2-4), 564–573.

Blouin, K. D., Flannigan, M. D., Wang, X., & Kochtubajda, B. (2016). Ensemble lightning prediction models for the province of alberta, canada. *International journal of wildland fire*, *25*(4), 421–432.

Boccippio, D. J., Williams, E. R., Heckman, S. J., Lyons, W. A., Baker, I. T., & Boldi, R. (1995). Sprites, elf transients, and positive ground strokes. *Science*, *269*(5227), 1088–1091.

Fleenor, S. A., Biagi, C. J., Cummins, K. L., Krider, E. P., & Shao, X.-M. (2009). Characteristics of cloud-to-ground lightning in warm-season thunderstorms in the central great plains. *Atmospheric Research*, *91*(2-4), 333–352.

Fuquay, D., Taylor, A., Hawe, R., & Schmid Jr, C. (1972). Lightning discharges that caused forest fires. *Journal of Geophysical Research*, *77*(12), 2156–2158.

Goodman, S. J., Blakeslee, R. J., Koshak, W. J., Mach, D., Bailey, J., Buechler, D., ... others (2013). The goes-r geostationary lightning mapper (glm). *Atmospheric research*, *125*, 34–49.

Krehbiel, P. R. (1981). An analysis of the electric field change produced by lightning. *Ph.D. Thesis*.

Lapierre, J. L., Sonnenfeld, R. G., Stock, M., Krehbiel, P. R., Edens, H. E., & Jensen, D. (2017). Expanding on the relationship between continuing current and in-cloud leader growth. *Journal of Geophysical Research: Atmospheres*, *122*(8), 4150–4164.

Li, S., Qiu, S., Shi, L., & Li, Y. (2020). Broadband vhf observations of two natural positive cloud-to-ground lightning flashes. *Geophysical Research Letters*, *47*(11), e2019GL086915.

López, J. A., Montanyà, J., van der Velde, O. A., Pineda, N., Salvador, A., Romero, D., ... Taborda, J. (2019). Charge structure of two tropical thunderstorms in colombia. *Journal of Geophysical Research: Atmospheres*, *124*(10), 5503–5515.

Mazur, V. (2002). Physical processes during development of lightning flashes. *Comptes Rendus Physique*, *3*(10), 1393–1409.

Montanyà, J., Van Der Velde, O., & Williams, E. R. (2014). Lightning discharges produced by wind turbines. *Journal of Geophysical Research: Atmospheres*, *119*(3), 1455–1462.

Nag, A., & Rakov, V. A. (2012). Positive lightning: An overview, new observations, and inferences. *Journal of Geophysical Research: Atmospheres*, *117*(D8).

Pu, Y., Cummer, S. A., & Liu, N. (2021). Vhf radio spectrum of a positive leader and implications for electric fields. *Geophysical Research Letters*, *48*(11), e2021GL093145.

Rakov, V. A., & Uman, M. A. (2003). *Lightning: physics and effects*. Cambridge university press.

Rison, W., Thomas, R. J., Krehbiel, P. R., Hamlin, T., & Harlin, J. (1999). A gps-based three-dimensional lightning mapping system: Initial observations in central new mexico. *Geophysical research letters*, *26*(23), 3573–3576.

Saba, M. M., Campos, L. Z., Krider, E. P., & Pinto Jr, O. (2009). High-speed video observations of positive ground flashes produced by intracloud lightning. *Geophysical research letters*, *36*(12).

Saba, M. M., Schulz, W., Warner, T. A., Campos, L. Z., Schumann, C., Krider, E. P., ... Orville, R. E. (2010). High-speed video observations of positive lightning flashes to ground. *Journal of Geophysical Research: Atmospheres*, *115*(D24).

Stock, M. (2014). *Broadband interferometry of lightning*. New Mexico Institute of Mining and Technology.

Stock, M., Akita, M., Krehbiel, P., Rison, W., Edens, H., Kawasaki, Z., & Stanley, M. (2014). Continuous broadband digital interferometry of lightning using a generalized cross-correlation algorithm. *Journal of Geophysical Research: Atmospheres*, *119*(6), 3134–3165.

Thomas, R. J., Krehbiel, P. R., Rison, W., Hunyady, S. J., Winn, W. P., Hamlin, T., & Harlin, J. (2004). Accuracy of the lightning mapping array. *Journal of Geophysical Research: Atmospheres*, *109*(D14).

Urbani, M., Montanyá, J., Van der Velde, O., López, J., Arcanjo, M., Fontanes, P., ... Roncancio, J. (2021). High-energy radiation from natural lightning observed in coincidence with a vhf broadband interferometer. *Journal of Geophysical Research: Atmospheres*, *126*(7), e2020JD033745.

van der Velde, O. A., Montanyà, J., Soula, S., Pineda, N., & Mlynarczyk, J. (2014). Bidirectional leader development in sprite-producing positive cloud-to-ground flashes: Origins and characteristics of positive and negative leaders. *Journal of Geophysical Research: Atmospheres*, *119*(22), 12–755.

Williams, E., Lyons, W., Hobara, Y., Mushtak, V., Asencio, N., Boldi, R., ... others (2010). Ground-based detection of sprites and their parent lightning flashes over africa during the 2006 amma campaign. *Quarterly Journal of the Royal Meteorological Society*, *136*(S1), 257–271.

Wu, T., Wang, D., & Takagi, N. (2020). Multiple-stroke positive cloud-to-ground lightning observed by the falma in winter thunderstorms in japan. *Journal of Geophysical Research: Atmospheres*, *125*(20), e2020JD033039.

Yuan, S., Qie, X., Jiang, R., Wang, D., Sun, Z., Srivastava, A., & Williams, E. (2020). Origin of an uncommon multiple-stroke positive cloud-to-ground lightning flash with different terminations. *Journal of Geophysical Research: Atmospheres*, *125*(15), e2019JD032098.

Zhu, Y., Bitzer, P., Rakov, V., Stock, M., Lapierre, J., DiGangi, E., ... Lang, T. (2021). Multiple strokes along the same channel to ground in positive lightning produced by a supercell. *Geophysical Research Letters*, *48*(23), e2021GL096714.